Polaronic-type excitons in ferroelectric oxides: Microscopic calculations and experimental manifestation

Valentin S. Vikhnin
A. F. Ioffe Physical Technical Institute, 194021, Saint-Petersburg, Russia

Roberts I. Eglitis, Siegmar E. Kapphan, and Gunnar Borstel
Universität Osnabrück–Fachbereich Physik, D-49069, Osnabrück, Germany

Eugene A. Kotomin
Institute of Solid State Physics, University of Latvia, 8 Kengaraga str., Riga LV-1063, Latvia
(Received 30 September 2001; revised manuscript received 3 December 2001; published 4 March 2002)

We discuss the current experimental and theoretical understanding of new polaronic-type excitons in ferroelectric-oxides charge-transfer vibronic excitons (CTVE's), which are pairs of strongly correlated electronic and hole polarons. It is shown that *charge-transfer–lattice distortion* interactions are the driving forces for CTVE formation. Hartree-Fock-type calculations performed in the framework of the intermediate neglect of differential overlap (INDO) method as well as photoluminescence, second-harmonic generation, and UV-absorption high-temperature studies performed for ABO_3 ferroelectric oxides strongly support the CTVE existence. Both single CTVE and a phase of strongly correlated CTVE's in their ferroelectric ground and antiferroelectric excited states are analyzed.

DOI: 10.1103/PhysRevB.65.104304 PACS number(s): 71.35.Aa, 71.38.Mx, 77.84.Dy

I. INTRODUCTION

Charge-transfer excitons interacting with the crystalline lattice have remained the subject of intensive theoretical studies during the last quarter of a century. The pioneering Agranovich-Reineker approach[1,2] was based on a linear exciton-phonon interaction which is induced by modulation of the Coulomb electron-hole attraction. Their basic assumptions are valid for many real systems but turn out to be nonadequate for ABO_3 ferroelectric oxides and other strongly polarizable partly covalent matrices with linear and significant *nonlinear vibronic interaction and anharmonicity*. The description of electronic excitations in these systems needs another approach. The development of such an approach is the main purpose of the present paper, the main idea of which is the charge-transfer vibronic exciton (CTVE).[3–7]

The CTVE in ABO_3 ferroelectric oxides with partly covalent chemical bonding consist of spatially well-correlated pairs of electronic and hole polarons.[3,4,8,9] The main driving force of the CTVE formation is an increase of the vibronic interactions due to a charge transfer from the O ion onto the B ion in ABO_3, characterized by the corresponding p and d pseudodegenerate and degenerate states which become reoccupied in the final, CTVE state. As the charge transfer exceeds some critical value, it induces *a local lattice instability* (the appearance of the maximum of the potential as a function of lattice distortion, Fig. 1). As a result, excited states with a new equilibrium charge transfer and lattice relaxation (relative minima of the potential) appear (Fig. 1) while the initial ground state remains stable with respect to the charge transfer-lattice effect. Note that an important opposite case of *charge-transfer–lattice distortion* local instability in the ground state can arise due to quasilocal charge-transfer-mode–quasilocal-vibration-mode repulsion.[10]

Strong vibronic energy reduction of CTVE's due to self-consistent lattice relaxation (up to ~ 3 eV in ABO_3 perovskites as we demonstrate below) can lead to the CTVE self-trapping. This is why the CTVE's could be treated also as intrinsic *deep centers* in their metastable state. That is, CTVE's can reveal the properties of low-mobile (via CTVE resonance cross relaxation[5]) intrinsic defects in oxygen-octahedrical perovskites and, probably, in general, in ferroelectric oxides characterized by partly covalent chemical bonding and vibronic interaction.

Note also that the CTVE state can be considered as a *bipolaron* comprising spatially correlated electron and hole polarons. Their correlation is defined by the *negative-U* effect.

Oxygen-octahedral ABO_3 perovskite ferroelectrics and related oxides serve as good examples of advanced materials with partly covalent chemical bonding, where, on the one

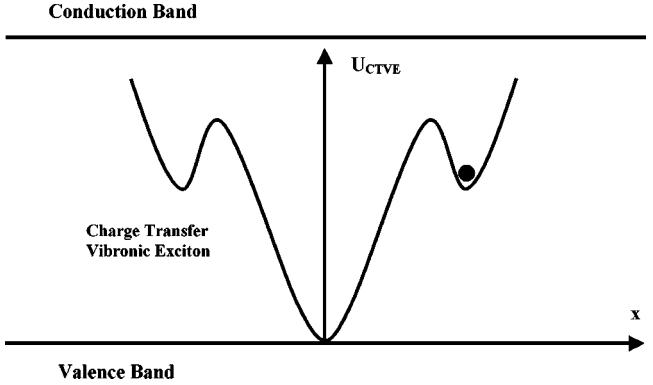

FIG. 1. The CTVE potential energy curve as a function of active-ion polar displacement with the charge-transfer–lattice interaction; anharmonic terms up to high order are included. This is the case of *charge-transfer–lattice distortion* instability in the anharmonic, excited state.

hand, charge-transfer effects are rather strong and, on the other hand, the vibronic interactions are also large. $KTaO_3$ (KTO) and $KNbO_3$ (KNO) crystals are considered below as illustrative examples of crystalline matrices revealing a new type of polaronic exitons (CTVE's) in ferroelectric and other oxides.

We present below quantitative arguments for CTVE formation which are based on microscopic intermediate neglect of differential overlap (INDO) calculations. Recently, this method was used very successfully in numerous studies of point defects and polarons in oxides and ferroelectrics.[11–18] Here we focus mainly on the charge-transfer effects in the CTVE, the atomic effective charges, and the local lattice distortions.

Special attention is paid to the idea of the existence of a *new* CTVE *phase* of ABO_3 crystals.[4,19] The CTVE phase is expected to consist of the strongly correlated CTVE's occupying *each* unit cell of a crystal. That is, in fact the CTVE phase corresponds to a new state of the crystal which is characterized by a new equilibrium charge transfer as well as new lattice parameters.

The plan of this paper is as follows. In Sec. II we discuss the peculiarities of the INDO method used in atomistic simulations. Section III is devoted to the treatment of the single CTVE including its charge transfer, lattice distortion, electronic, and vibronic (Jahn-Teller effect) properties. The CTVE parameters obtained confirm the existence of such type excitations and their uncommon properties. Section IV presents quantitative arguments for the CTVE phase existence which are based on careful microscopic INDO calculations. In particular, we calculate the effective charges and lattice distortions characterizing the CTVE phase. The experiments which verificate the CTVE existence, including the single CTVE as well as the CTVE phase, are discussed in Sec. V. These experiments are based on the optical properties of the ABO_3 ferroelectric oxides: namely, photoluminescence (PL), temperature dependence of fundamental light absorption edge (FLA), and the second-harmonic generation (SHG) efficiency.

II. COMPUTATION METHOD

Ab initio methods are still cumbersome and time consuming for the treatment of the electronic and atomic structure of complex systems, especially those with partially covalent chemical bonding, like ABO_3 perovskites. In order to be able to study relatively complicated cases of perovskite solid solutions, defects, and excitons, there is a strong need to close the gap between accurate but time-consuming *ab initio* methods[20–26] and widely used, simple but not so accurate *ad hoc* parameter-dependent phenomenological approaches. A possible compromise is to use some semiempirical quantum chemical method with transferable parameters valid for a wide class of systems. An example of such a method is the modified INDO method,[15,16] which is a semiempirical version of the Hartree-Fock method.

The Fock matrix elements in the modified INDO approximation[15,16] contain several semiempirical parameters. The first one is the orbital exponent ζ entering the radial part of Slater-type atomic orbitals:

$$R_{nl}(r)=(2\zeta)^{n+1/2}[(2n)!]^{-1/2}r^{n-1}\exp(-\zeta r), \qquad (1)$$

where n is the principal quantum number of the valence shell. We used here a valence basis set including $4s$, $4p$ atomic orbitals (AO's) for K, $2s$, $2p$ for O, $5s$, $5p$, $4d$ for Nb, and $6s$, $6p$, $5d$ for the Ta atom. The diagonal matrix elements of the interaction of an electron occupying the μth valence AO on atom A with its own core are taken as

$$U^A_{\mu\mu}=-E^A_{\rm neg}(\mu)-\sum_{\nu\in A}\left(P^{(0)A}_{\nu\nu}\gamma_{\mu\nu}-\frac{1}{2}P^{(0)A}_{\nu\nu}K_{\mu\nu}\right), \qquad (2)$$

where $P^{(0)A}_{\mu\mu}$ are the diagonal elements of the density matrix, and $\gamma_{\mu\nu}$ and $K_{\mu\nu}$ are one-center Coulomb and exchange integrals, respectively. The parameter $E^A_{\rm neg}(\mu)$ is the μth AO energy. The matrix elements of interaction of an electron on the μth AO belonging to atom A with the core of another atom B are calculated as follows:

$$V^B_\mu=Z_B\{1/R_{AB}+[\langle\mu\mu|\nu\nu\rangle-1/R_{AB}]\exp(-\alpha_{AB}R_{AB})\}, \qquad (3)$$

where R_{AB} is the distance between atoms A and B, Z_B is the core charge of atom B, and α_{AB} is an adjustable parameter characterizing the finite-size effect of the atomic core B and additionally the localization of the μth AO. The quantity $\langle\mu\mu|\nu\nu\rangle$ is the two-center Coulomb integral. The resonance integral parameter $\beta_{\mu\nu}$ enters the off-diagonal Fock matrix elements for the spin component $u=\alpha,\beta$:

$$F^u_{\mu\nu}=\beta_{\mu\nu}S_{\mu\nu}-P^u_{\mu\nu}\langle\mu\mu|\nu\nu\rangle, \qquad (4)$$

where the μth and νth AO's are centered at different atoms, $S_{\mu\nu}$ is the overlap matrix between them, and $\langle|\rangle$ denotes two-electron integrals.

In the last decade the INDO method has been successfully used for bulk solids and defects in many oxides[15,16] and semiconductors.[17] This method has been earlier applied to the study of phase transitions and frozen phonons in pure KNO,[12] pure and Li-doped KTO,[13] point defects in KNO,[11] and solid perovskite solutions $KNb_xTa_{1-x}O_3$ (KTN),[18] as well as F centers and hole polarons in KNO.[11,14]

A detailed analysis of the development of the INDO parametrization for pure KNO and KTO is given in Refs. 12 and 13. The INDO method reproduced very well both available experimental data and results of *ab initio* local-density-approximation-type (LDA-type) calculations. In particular, this method reproduces the effect of a ferroelectric instability of KNO due to off-center displacement of Nb atoms from the regular lattice sites, as well as the relative magnitudes of the relevant energy gains for the [100], [110], and [111] Nb displacements. These are consistent with the sequence of the stability of the tetragonal, orthorhombic, and rhombohedral ferroelectric $KNbO_3$ phases, respectively, as the crystal's temperature decreases. This is a very nontrivial achievement since the typical energy gain due to the Nb off-center displacement is only of the order of several mRy per unit cell.

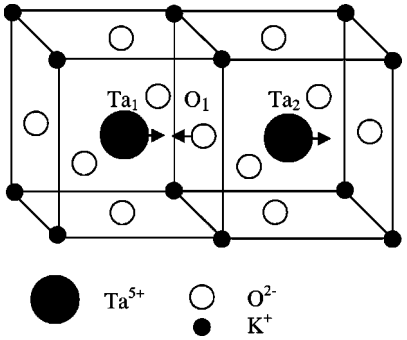

FIG. 2. The INDO-calculated triad atomic structure of the CTVE in KTO. The displacements of three active Ta-O-Ta ions constituting the triad center are shown.

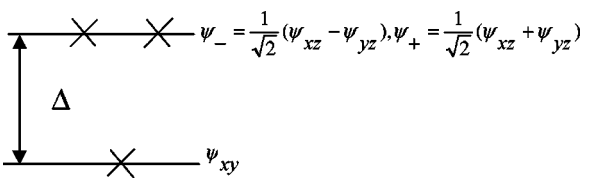

FIG. 3. The scheme of Ta $5d$ atomic states occupied in the self-trapped CTVE. Δ is the energy splitting due to the axial internal field caused by the CTVE self-trapping. The state degeneracy is noted by number of crosses.

The calculated frequencies of the transverse-optic (TO) phonons at the Γ point in the Brillouin zone (BZ) of cubic and rhombohedral KNO, and the atomic coordinates in the minimum energy configuration for the orthorhombic and rhombohedral phases of KNO, are also in good agreement with experiment, thus indicating that a highly successful INDO parametrization has been achieved. The frozen-phonon calculations for T_{1u} and T_{2u} modes of cubic KTO are also in good agreement with experiment. Appreciable covalency of the chemical bonding is seen from the calculated (static) effective charges on atoms (calculated using Lowdin population analysis): $0.62e$ for K, $2.23e$ for Ta, and $-0.95e$ for O in KTO, which are far from those expected in the widely used ionic model ($+1e$, $+5e$, and $-2e$, respectively). These charges show slightly higher ionicity in $KTaO_3$ as compared with the relevant effective charges calculated for KNO: $0.54e$ for K, $2.02e$ for Nb, and $-0.85e$ for O.

III. CALCULATIONS OF THE ATOMIC STRUCTURE

A. INDO calculations

The important CTVE feature is the charge-transfer effect which is self-consistent with the accompanied lattice distortion. The computations of the electronic and distorted lattice structure for the CTVE in KTO were performed by means of the INDO method using the periodic supercell model where the primitive KTO unit cell volume was extended by a factor of $3\times3\times3=27$. As a result, the following structure was obtained as shown in Fig. 2: the CTVE has a *triad* atomic structure with a strong vibronic energy reduction (~2.71 eV). This is connected with the hole polaron localization on one oxygen ion which is displaced by 5.2% of the lattice constant towards the (first) active Ta ion on which the electronic polaron is mainly localized. In its turn, this first active Ta ion has a 3.1% displacement towards the oxygen ion. However, the second active Ta ion, on which the electron polaron is also partly localized, reveals a 4.5% *outwards* displacement, due to a repulsion from the active oxygen—in a contrast to the first Ta ion. The final charge distribution inside the triad Ta-O-Ta is the following: the first Ta ion has an effective charge of $1.74e$, while the second Ta ion has $2.12e$ and an active oxygen ion $-0.24e$. Thus, the corresponding equilibrium charge-transfer value towards the first Ta ion is $-0.49e$, the second Ta ion is $-0.11e$, and *from* the active oxygen ion is $0.71e$. The effective Mulliken charges of Ta and O in *perfect* KTO ($2.23e$ and $-0.95e$) clearly demonstrate strong covalent Ta-O bonding.

The charge-transfer and corresponding lattice distortion inside the CTVE are rather large and controlled by the strong vibronic interaction. Note that vibronic instability appears already at essentially smaller magnitudes of the charge transfer and lattice distortion. That is, the ground CTVE state lies outside the instability region.

The energy level of the electronic polaron shared by the two Ta ions in KTO lies by ~0.8 eV below the bottom of the conduction band, whereas the energy level of the hole polaron is localized on the oxygen ion by ~1 eV above the top of the valence band. The hole-polaron wave function consists mainly of the active O $2p_z$ atomic orbital directed towards the first Ta ion (the CTVE's z axis); however, the electronic structure of the electronic polaron within CTVE is more complicated. Namely, there are three Ta (t_{2g}) states: the nondegenerate ground state and twofold-degenerate low-lying excited state (see also the next section, Sec. III B, and Fig. 3). The ground state consists of $5d_{xy}$ atomic orbitals of the first Ta [with the molecular-orbital linear combination of atomic orbitals (MO-LCAO) coefficient ~0.344], of the second (coefficient 0.162), and contribution of all other Ta ions (with coefficients strongly decreasing with the distance from the triad). The double-degenerate low-lying excited state contains mostly $5d_{xz}$ and $5d_{yz}$ atomic orbitals, respectively, with coefficients 0.231 for the first Ta and ~0.150 for the second Ta. The self-consistent lattice distortion rapidly decreases with distance from the triad Ta_1-O-Ta_2. The calculations presented here confirm the first evidence of the triad structure of the CTVE in KTO suggested in Ref. 8. A similar triad structure of the CTVE was calculated later for KNO.[9]

Of special importance is the CTVE magnetic structure. The present INDO calculations show that the triplet ($S=1$) CTVE state is the *ground* state, while the singlet ($S=0$) is the excited state, with a small excitation energy of ~0.07 eV (in KTO). The relaxation energy is slightly lower for the singlet state (~2.64 eV) than for the triplet state. The triad-core lattice displacements and charge transfer are similar for the singlet and triplet states. Indeed, the Ta_1 ion has an effective charge of $1.78e$ (charge transfer $-0.45e$) and is displaced towards the active O by 3.0%, while Ta_2 has the effective charge of $2.13e$ (and charge transfer $-0.10e$) with a 4.35% outward displacement from the active O ion.

This active O has effective charge $-0.27e$ (charge transfer is $0.68e$) and reveals the 5.05% displacement towards the Ta_1 ion.

From the INDO calculations the general conclusion can be drawn that the CTVE has a well-defined atomistic triad structure, characterized by a deep in-gap energy position of local electronic states, accompanied by a strong self-consistent local lattice distortion. It is important that in KTO the singlet CTVE state has a little bit smaller binding energy than the triplet CTVE state. This is the low-lying nonmagnetic excited state which can be easily thermally populated, even at room temperature.

B. Role of the Jahn-Teller effect

The Ta $5d$ states of the CTVE have a nondegenerate ground ψ_{xy} state and low-lying degenerate excited states ψ_{xz}, ψ_{yz}. According to our INDO calculations, the corresponding Δ splitting of the t_{2g} state (Fig. 3), being induced by a tetragonal Q_{zz} field, is ~ 0.009 eV. This triplet state can be active in the Jahn-Teller effect (JTE) and also in a pseudo-Jahn-Teller effect associated with the active low-symmetry lattice distortions different from Q_{zz} and Q_z which we used above as the basic CTVE lattice distortions.

Let us consider the JTE on the Q_{xy}, $Q_{x^2-y^2}$ trigonal and tetragonal distortions. The corresponding linear vibronic interaction is defined by the following Hamiltonian:

$$H_{vibr.}=A\hat{\varepsilon}_{xy}Q_{xy}+B\hat{\varepsilon}_{x^2-y^2}Q_{x^2-y^2}, \tag{5}$$

where $\hat{\varepsilon}_{xy}$ and $\hat{\varepsilon}_{x^2-y^2}$ are the electronic operators on the basis of $5d_{ij,i\neq j}$ states, Q_{xy}, $Q_{x^2-y^2}$ are local CTVE distortions of the same symmetry as above-mentioned electronic operators, and A,B are vibronic interaction parameters.

It should be noted that Eq. (5) describes the vibronic effects only for the low-lying excited doublet state (Fig. 3). This expression can be rewritten in terms of Pauli matrices σ_z and σ_x on the basis of Ψ_+, Ψ_- wave functions (Fig. 3). As a result, we get $H_{vibr}=A\hat{\sigma}_z Q_{xy}+B\hat{\sigma}_x Q_{x^2-y^2}$. This leads, in the strong JTE approach, to an adiabatic potential of the following form:

$$U_{ad.}=\frac{m_\varepsilon\omega_\varepsilon^2 Q_{x^2-y^2}^2}{2}+\frac{m_{xy}\omega_{xy}^2 Q_{xy}^2}{2} \pm\sqrt{(AQ_{xy})^2+(BQ_{x^2-y^2})^2}, \tag{6}$$

where the two first terms are potential energies of $Q_{x^2-y^2}$ and Q_{xy} vibrations in the harmonic approximation, and the last term is of vibronic origin. The minimization of this expression with respect to $Q_{x^2-y^2}$ (i) and Q_{xy} (ii) distortions gives only two types of two-well potentials with minima, respectively, at

$$Q_{x^2-y^2}=0, \quad Q_{xy}=\pm\frac{A}{m_{xy}\omega_{xy}^2}(i),$$

$$Q_{xy}=0, \quad Q_{x^2-y^2}=\pm\frac{B}{m_\varepsilon\omega_\varepsilon^2}. \tag{7}$$

It should be noted that the $Q_{x^2-y^2}$ minima of the two-well potential correspond to Ψ_{xz} and Ψ_{yz} electronic wave functions, whereas the Q_{xy} minima correspond to the Ψ_+ and Ψ_- electronic functions mentioned above. The Jahn-Teller ground state corresponds to one of these two types vibronic two-well states. The type of ground vibronic state is determined here by the largest Jahn-Teller energy among these two vibronic configurations.

Let us discuss the situation where Q_{xy} minima give rise to the ground vibronic state while $Q_{x^2-y^2}$ minima give rise to the excited state. In the framework of the strong JTE (due to the random field effect) CTVE self-trapping can lead to an occupation of only one of the two Q_{xy} minima in the ground state. This corresponds to an occupation of Ψ_{xy}, Ψ_+ or Ψ_{xy}, Ψ_- d states. As a result, the CTVE turns out to be affected not only by strong tetragonal and polar fields, but also the Jahn-Teller *trigonal* field. This is in good agreement with an experimental magneto-optical study[27] of the center responsible for the *red* luminescence in KTO discussed in Sec. V. Therefore, based on our calculations, we predict that a single CTVE is not of high C_{4v} symmetry, but is characterized by a definite equilibrium Q_{xy} distortion of the lower C_{2v} symmetry. This is a consequence of the strong Jahn-Teller effect on active CTVE d states.

IV. NEW CRYSTALLINE PHASE OF CHARGE-TRANSFER VIBRONIC EXCITONS

A. INDO calculations for the CTVE phase in the ferroelectric ground state

Let us return now to the idea of the *new* CTVE *crystalline phase* in ferroelectric perovskites.[3,4] This phase is expected to consist of the strongly correlated CTVE's which are located in *each* unit cell of the ABO_3 crystal. That is, in fact the CTVE phase corresponds to a new state of the crystal which is characterized by a new equilibrium charge transfer as well as new lattice parameters.

The first step in the theoretical study of the CTVE *phase* was done in Ref. 4 using a semiphenomenological model. This model dealt with point dipoles corresponding to equilibrium displacements in the CTVE cell which gives *the order parameter* for the CTVE phase as well as with electronic degrees of freedom of CTVE active ions assuming electronic state degeneracy or pseudodegeneracy. These two interacting degrees of freedom also interact with other lattice distortions (polarization and deformation). It was shown there that an important role in the CTVE phase formation belongs to a specific vibronic interaction characterized by a direct coupling of charge transfer with lattice distortions, both in the linear and nonlinear approximations. According to these estimates, the CTVE phase energy position[4] lies inside the gap of a perfect crystal, but rather close to its valence band top. However, a direct, nonmodel computation of CTVE phase properties is obviously needed which was performed here by means of the quantum-chemical INDO method and using the

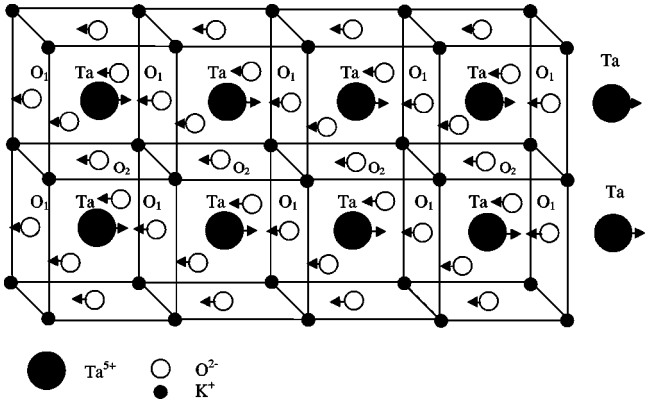

FIG. 4. The sketch of the structure of the charge transfer vibronic exciton phase in its ferroelectric ground state.

same $3\times3\times3$ extended large unit cell as before. Our INDO calculations demonstrate that the novel CTVE phase could really exist in the well-known incipient ferroelectric KTO.

(i) The triplet CTVE phase in the ground state was obtained as a ferroelectric phase with parallel-oriented spins of small-polaron electron-hole pairs localized on O-Ta ions and producing rather deep in-gap states. Indeed, the total energy gain per such a O-Ta pair was very considerable, 2.32 eV, for the ferroelectric phase ground state. Such a large value of the relaxation energy arises due to a strong vibronic interaction. It indicates the CTVE-phase level decrease in energy with respect to noncorrelated electron-hole pairs. Namely, this large potential barrier must be overcome for the CTVE-phase decay. (ii) The equilibrium displacements of O-Ta ions in each electron-hole pair are directed towards each other and are rather large: 4.33% for the Ta ion and 5.62% for the O ion. The self-consistent charge transfer is also large, $-0.77e$, accompanied by the equilibrium effective charge of $1.46e$ for the Ta ion, whereas for the O ions they are $0.77e$ and $-0.18e$, respectively. Note that ferroelectrically ordered oxygen ions in the intermediate chains relatively to O-Ta CTVE chains are much less shifted (0.37%) in the same direction as oxygen ions in the CTVE chains (Fig. 4). (iii) The CTVE-CTVE correlation energy (the energy gain per the electronic-hole pair due to the CTVE-CTVE interaction) within the CTVE phase can be estimated to be 0.5 eV.

Note that the similarity of the parameters of individual CTVE's and the CTVE phase can be understood on the basis of the large magnitude of the relaxation energy per CTVE pair relative to the correlation energy for the CTVE-CTVE interaction within the CTVE phase.

Another model example, characterized by slightly higher bonding covalency, is KNO. The parameters of the ferroelectrically ordered CTVE phase were calculated here on the basis of the same INDO approach as for KTO. The total energy gain per O-Nb pair is smaller, 1.99 eV. However, this also corresponds to the case of a strong vibronic interaction, which is slightly decreased due to a small increase in the chemical bond covalency. The equilibrium displacements of O-Nb ions in each polaronic electron-hole pair are also directed towards each other and remain rather large: 4.15% for the Nb ion and 5.28% for the O ion. Self-consistent charge transfer is also considerable $-0.70e$ (the equilibrium effective charge $1.32e$) for the Nb ion, and $0.70e$ (with an equilibrium effective charge $-0.15e$) for the O ion in the CTVE chains. Oxygen ions in the intermediate chains reveal a 0.35% shift parallel to that of oxygen ions in the CTVE chains. Thus, the INDO calculations for KTO and KNO confirm a high stability of the CTVE phase in ferroelectric oxides.

The electronic structure of the CTVE phase is in some respects similar to that of a single CTVE. Indeed, the position of the electronic polaron level in KTO is 1 eV below the conduction band, while in KNO it is 0.9 eV, both parameters corresponding to the CTVE phase. Simultaneously, the hole level in the CTVE phase of KTO lies by 1.2 eV above the valence band top, while in CTVE phase of KNO it is located at 1.1 eV above the valence band top.

We estimate the width of the CTVE conduction band as well as the width of the CTVE valence band to be ~1 eV. The latter estimate is based on model calculations (see, e.g., Ref. 28) of the electronic matrix elements between orbitals of oxygen ions and B ions of ABO_3 perovskites. Taking into account this estimate, as well as above-mentioned electron and hole level positions within the CTVE phase found by means of INDO calculations, we can make the following suggestions about CTVE conduction and CTVE valence band edge positions. Namely, the noncontradictory positions of these CTVE band edges could be very close to the corresponding band edges of normal, nonexcitonic states of a perfect ABO_3. That is why we can assume that the normal conduction band and the CTVE conduction band slightly overlap, while the corresponding valence bands do not overlap but have a rather small gap between the bottom of the CTVE valence band and the top of the normal valence band (Fig. 5). Namely, these (quite reasonable) assumptions allow us to explain the unusually strong temperature behavior of the FAE in SBN and in KTO ferroelectric oxides as it will be shown in Sec. V.

It should be stressed that a strongly polarized ferroelectric phase exists in the ground CTVE state. Thus we can expect that the real CTVE phase is the multidomain state where domain walls can move due to successive CTVE reorientations due to a resonance cross-relaxation process. Additionally, we have evaluated the CTVE-phase state constructed from the *triplet* spin states of individual CTVE's. The latter are based on the above-presented INDO calculations of the singlet-triplet splitting for an individual CTVE and on the assumption that the CTVE-CTVE spin-spin interaction does not change such a spin order. While this evaluation confirms that the *triplet* spin state is a real ground state of an individual CTVE in KTO and, probably, in related systems, the CTVE-CTVE spin-spin interaction effect can lead to many-variant magnetic structures for the CTVE phase. For instance, if the polaronic electron-electron and hole-hole interactions can be significantly antiferromagnetic, the resulting antiferromagnetic structure will dominate the CTVE-phase ground state. The latter is really the case for the ferroelectric oxides under consideration. Taking into account the antiferromagnetic coupling between spins of two electronic polarons via intermediate oxygen ions, as well as be-

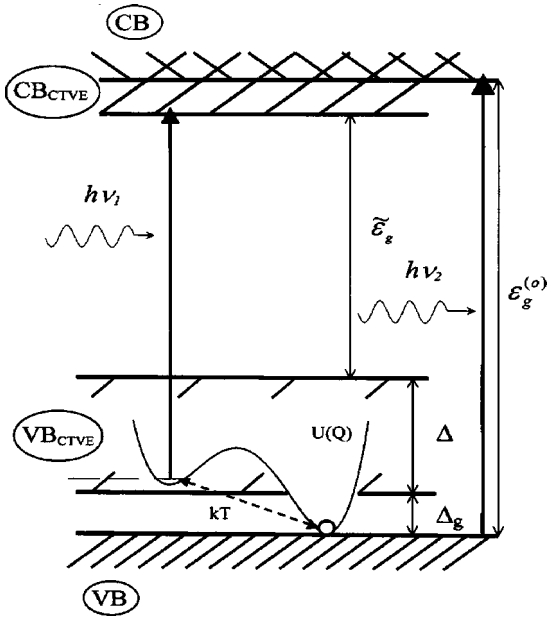

FIG. 5. The *normal* band structure including the new CTVE-phase bands. CB, VB, and $\varepsilon_g^{(0)}$ are the normal-state conduction band, valence band, and corresponding band gap; CB_{CTVE}, and VB_{CTVE} are conduction and valence bands of the CTVE phase, $U(Q)$ is the adiabatic potential vs active lattice displacement, Δ the VB_{CTVE} width; two new band gaps are also marked. Thermal excitation $VB \rightarrow VB_{CTVE}$ and following $VB_{CTVE} \rightarrow CB_{CTVE}$ optical absorption transition are noted which are characterized by a drastic redshift of the wavelength.

tween spins of two hole polarons via intermediate *B* ions for oxygen-octahedrical perovskite-like systems, the antiferromagnetic state could become a ground magnetic state for the CTVE pair. An extension of this conclusion leads to the idea that the CTVE phase also becomes antiferromagnetic.

As was shown above, the magnetic properties of the CTVE phase can be related not only to spin-related degrees of freedom. Namely, the electronic orbital moments of the *d* states of *B* ions in the CTVE become important if the Jahn-Teller effect on these *d* states is not very strong, and the vibronic reduction effect is small. In general, the competition of spin and orbital moments is possible. This can lead to the incommensurate magnetic ordering, as well as to two limiting cases of ferro- and antiferromagnetic ordering. Nevertheless, we consider here another approach with the strong Jahn-Teller effect on *d* states of *B* ions with a correspondingly strong vibronic reduction. As a result, only spin magnetic moments become important in the framework of this problem.

As follows from the last conclusion, photo- and thermo-induced antiferromagnetic resonance could serve as the effective methods for a study of the CTVE phase.

B. Long-range interaction contribution to CTVE-phase formation

It should be noted that evaluation of the CTVE-phase relaxation energy per O-Ta pair in the framework of finite large unit cells (like the $3\times3\times3$ extension used in our INDO calculations) gives us only the contribution of the short-range and of the middle-range interactions which contribute to the CTVE-phase formation. However, in some cases this is not sufficient. Namely, the long-range forces are also important in ferroelectric-type ordered states, like the CTVE phase in its ground state discussed above. The CTVE's exist in the long-range polarization field $\mathbf{P}_{\mathbf{k}=\mathbf{0}}$, which is the *order parameter*. This polarization field directly interacts with three types of point electric dipoles (see Fig. 4), related in the KTO case to the Ta ion ($\mathbf{d}_1$), with the O_1 ion in the same [100] chain along the polarization direction ($\mathbf{d}_2$) and with the O_2 ion in the intermediate [100] chain without Ta ions ($\mathbf{d}_3$). All these three dipoles have the same direction (along the $\mathbf{P}_{\mathbf{k}=\mathbf{0}}$ field) and interact with this polarization via the *local field*, $\mathbf{E}_{loc}^{i}=(4\pi/3)\gamma_i\mathbf{P}_{\mathbf{k}=\mathbf{0}}$, where γ_i is the local field factor of the ith type of active ion. As a result, the total relaxation energy per unit cell of the CTVE phase in its ferroelectric ground state can be presented as

$$\varepsilon_{total}=\varepsilon_{short\text{-}range}-(4\pi/3)\mathbf{P}_{\mathbf{k}=0}(\mathbf{d}_1\gamma_1+\mathbf{d}_2\gamma_2+2\mathbf{d}_3\gamma_3), \tag{8}$$

where $\varepsilon_{short\text{-}range}$ is the short-range contributions to the relaxation energy of the CTVE phase. Taking into account the values of the $\mathbf{P}_{\mathbf{k}=0}$, the $\mathbf{d}_1$, $\mathbf{d}_2$, and $\mathbf{d}_3$ parameters obtained on the basis of the INDO calculations presented above, as well as $\gamma_1\approx5.28$ (for the Ta ion), $\gamma_2\approx3.78$ (for the O_1 ion), $\gamma_3\approx0.22$ (for the O_2 ion) values[29] of local field factors for KTO, for example, we obtain that the second, long-range contribution in Eq. (8) corresponds to the relaxation energy of 0.454 eV. Thus, the resulting relaxation energy per unit cell for the ferroelectric ground state of the CTVE phase becomes as large as -2.77 eV. The long-range contribution to this total energy is rather pronounced ($\approx16.4\%$). Very similar results are obtained also for the CTVE phase in KNO (with a $\sim14\%$ difference from KTO).

C. Antiferroelectric CTVE phase in the excited state

Naturally, the above-considered ferroelectric structure of the ground CTVE-phase state is not the only possible state for the CTVE phase. There are many different excited CTVE-phase states with different geometries (see, e.g., the structures of the corresponding CTVE-phase clusters[3]). One of them is the *antiferroelectric* CTVE phase. Such a phase consists of ferroelectric chains with antiferroelectric ordering (Fig. 6). Let us calculate its parameters for the KTO crystal. The relaxation energy includes here only the short-range and the middle-range contributions which were evaluated within our INDO approach. As a result, one gets $\varepsilon_{total}=\varepsilon_{short\text{-}range}=-2.17$ eV per pair, and the energy difference between antiferroelectric excited and ferroelectric ground CTVE-phase states is 0.62 eV. According to our INDO calculations, the correlation CTVE-CTVE energy in the antiferroelectric CTVE phase (attraction) is a little bit smaller than in the ferroelectric state and equals -0.35 eV for KTO. The equilibrium charge transfer from the O_1 to the Ta_1 ion is large, $-0.73e$. As a result, the effective charges on these ions become $-0.22e$ and $1.50e$, respectively.

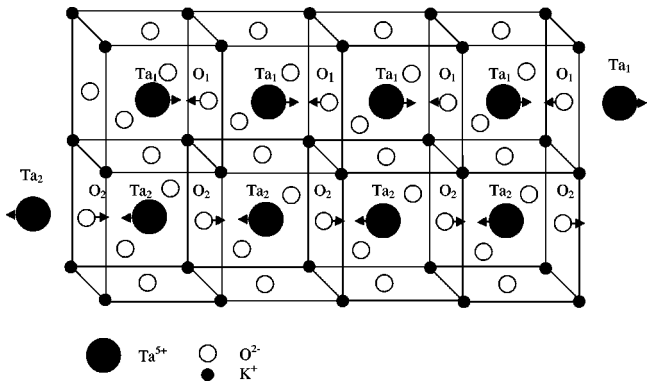

FIG. 6. The structure of the charge-transfer vibronic exciton phase in its excited antiferroelectric state.

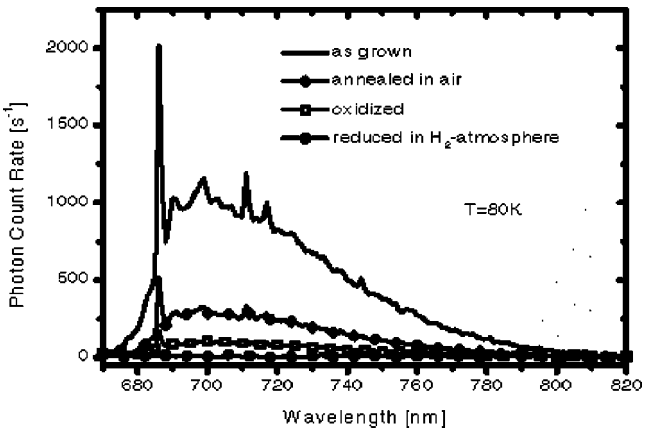

FIG. 7. The spectrum of red luminescence of nominally pure KTO, as grown and after three different types of thermal treatment.

Last, the lattice distortion, self-consistent with the charge transfer, takes place in the antiferroelectric CTVE phase. It is also very significant and similar (within corresponding ferroelectric chains) to an analogous lattice distortion in the ferroelectric CTVE phase. Here the O_1 and Ta ions have 5.48% and 4.15% displacements (in units of the lattice constant), respectively, which are directed towards each other. Last but not least, the antiferroelectric CTVE phase in KTO is characterized by slightly more shallow electronic and hole levels of the CTVE-phase-correlated states in comparison with the corresponding ferroelectric phase. Namely, the electronic level is below the conduction band edge by 0.92 eV, while the hole level is above the valence band gap edge by 1.13 eV. These energies of polaronic origin are very similar for ferro- and antiferro-CTVE phases as well as for the single-CTVE case. It should be underlined that IR *optical transitions* (with quantum energy approximately equal to 0.62 eV) between antiphase boundaries of the domains in the CTVE-phase ferroelectric ground state, on the one hand, and in the CTVE-phase antiferroelectric excited state, on the other hand, can be rather effective. The latter is due to approximate coincidence of the lattice distortions for these initial and final states.

Let us discuss now experimental manifestations of the single-CTVE and CTVE phases.

V. EXPERIMENTAL CTVE MANIFESTATIONS

A. Red luminescence as a result of radiative CTVE recombination

According to experiments, there are *two* characteristic excitonic luminescence energies observed in KTO: the luminescence band at 1.8–1.9 eV,[27,30–32] the so-called *red* luminescence (RL), and another band with a larger quantum energy[6,33] (around 2.6–2.7 eV), the so-called *green* luminescence (GL). GL was also detected in $SrTiO_3$,[34,35] in Li-doped $KTaO_3$,[36] and in $KNbO_3$.[37] As it was suggested in Ref. 6 for the case of GL and in the Ref. 32 for the case of RL, both bands arise as a result of the CTVE radiative recombination. Since the GL signal in KTO crystal is strongly dependent[6] on the thermal treatment (reduction or oxidation), the corresponding CTVE recombination center could be of more complicated structure than just a single CTVE. Indeed, the natural assumption could be that GL arises due to a radiative recombination of the CTVE trapped by an oxygen-related defect (e.g., oxygen vacancy[6]). However, identification of the actual defect involved in this case needs additional experimental confirmation. The situation with RL is also rather uncommon but in this case we have some reasons to assume a manifestation of a *pure* single CTVE. Let us discuss this case in more detail.

Indeed, as was supposed,[31] the RL arises due to some intrinsic centers of nonimpurity nature which disappear under heat treatment (Fig. 7). This supports the assumption[32] that RL in KTO is the CTVE recombinational luminescence because the CTVE is a metastable intrinsic quasicenter (due to a bipolaron self-trapping in the strong field of the lattice distortion). It should be stressed that the proposed model[32] predicts the total angular moments $J=2$, $J=1$, and $J=0$ for the *triplet-spin* state of the CTVE. This is true for a strong enough spin-orbit interaction mixing the CTVE triplet-spin state (a sum of 1/2 spins of the electron and hole polarons) and a quasidegenerate orbital triplet comprising Ta $5d$ states. The characteristic structure of the RL spectrum with three narrow lines[27,31,32] could be easily explained in this model by the optical transitions from the above-mentioned $J=2$, $J=1$, and $J=0$ states. Note that the contribution of the $(5d^2)Ta^{3+}$ electronic state near the oxygen vacancy to the RL active state assumed in Refs. 27 and 31 is not principally necessary for an explanation of RL experiments. But the JTE analysis in the framework of the model proposed can explain some additional RL peculiarities. For instance, our JTE model is useful for understanding the nature of the trigonal field detected in the experiments on the RL recombination center.[27] This field could be induced by the JTE on the orbital triplet's $5d$ state of the active Ta ion involved in the CTVE as considered above. Now let us discuss some RL peculiarities.

(i) The observed rather long lifetime of the RL, ~ 3.4 ms, within the temperature range of $T=15$–60 K (Ref. 30) is also in agreement with the CTVE radiative recombination mechanism and could be caused by a strong local lattice distortion around the above-considered atomic triad of the spatially correlated electronic and hole polarons. (ii) Another circumstance is connected with RL excitation spectrum pe-

culiarities. The CTVE recombination model can explain it as an effect of the occupation of the CTVE excited states with their following relaxation to the CTVE ground state active in the RL. (iii) RL thermal quenching is observed at $T > 100$ K, but the RL intensity maximum is observed at ~ 75 K. The latter can be explained as a result of the specifics of the RL which takes place under the conditions of a strong vibronic reduction. This circumstance makes effective nondirect, two-step mechanism of the RL. Namely, the first step is the thermal excitation with an occupation of the CTVE excited vibrational state which has enough overlapping with the ground-state system (the corresponding vibrational energy for such an excitation can be ~ 75 K). The CTVE recombination at the second step takes place with participation of the excited vibrational CTVE state mentioned above. (iv) Last, but not the least, the strong dependence of the RL from all kinds of thermal treatments could be understood as a result of a strengthening of the CTVE mobility due to thermal increase of the CTVE cross-relaxation rate. The latter leads to a significant decrease of the number of free CTVE's due to a large cross section for CTVE trapping by electric (elastic) dipole defects. The trapping by defects strongly changes the CTVE structure, up to a vanishing of the RL. Thus, we assume that the single CTVE active in the RL should exist only in pure enough samples (Fig. 7).

It should be noted that our INDO calculations for electron-hole polaron radiative recombination inside the CTVE performed for pure KTO (Ref. 9), predict a luminescence energy of ~ 2.12 eV. This value is only by ~ 0.2–0.3 eV larger than the quoted experimental RL energy, which lies in the limits of the computational accuracy of the method.

The CTVE could be also effectively studied using *magnetic resonance* techniques. First of all, there is photoelectron paramagnetic resonance (photo-EPR) in $J=1$ and $J=2$ CTVE states in KTO and KNO under the illumination-induced occupation of these excited states. In contrast, the $J=0$ ground state of the CTVE is nonmagnetic and thus EPR silent.

B. Green luminescence of bound CTVE's

Along with the discussed GL observed in the nominally pure incipient ferroelectric KTO, this was observed also in other crystals like $SrTiO_3$ and in KTO doped with off-center Li^+ ions (KLT system).

(i) The CTVE recombination concept was found applicable also for the case of other partly covalent ferroelectric perovskites like $SrTiO_3$.[34,35] No excitonic absorption was observed here (the excitation spectrum was assumed to be located in the band-band transition region) but the luminescence spectrum with the peak at 2.4 eV indicates the existence of self-trapped excitons. Such excitons arise due to hopping motion and coupling of electronic and hole polarons, which is supported by the analysis of time-resolved luminescence spectra. The self-trapped exciton nature is confirmed by its broad bandwidth (0.5 eV) and the large Stokes shift (0.8 eV). All these data are in good agreement with the CTVE model. The reduction treatment of the sample increases the luminescence signal and supports the assumption that we again deal with the complex *CTVE-oxygen-related defect*.

(ii) A more stable CTVE is observed in KTO doped with strongly reorienting dipole impurities. Indeed, we observe here self-consistent CTVE and dipole-impurity orientations which correspond to a maximum magnitude of the *CTVE dipole-impurity dipole* mutual attraction. Such an attraction has three origins. First, there exists an electrical, dipole-dipole interaction between point dipoles within the CTVE and point dipole of the impurity. Second, there is an elastic dipole-dipole interaction. Last but not least, there are two cross-type electric-dipole–elastic-dipole interactions between the CTVE and dipole impurity via electrostriction. They also take place between the CTVE and dipole impurity. Such a case corresponds to $K_{1-x}Li_xTaO_3$ (KLT) which consists of the CTVE-related dipole system, on the one hand, and off-center Li^+ ion dipole moments, on the other hand. The CTVE-Li^+ stable pairs appear here, as well as CTVE clusters with Li^+ ions as their cores. As a result, the CTVE recombinational luminescence intensity and thermal stability increase. Such effect was indeed detected experimentally.[36]

(iii) It should be stressed that detected x-ray-excited low-temperature GL in KNO with a well-defined peak at ~ 2.15 eV (Ref. 37) could be interpreted as a result of recombination of nearly free CTVE taking into account a good agreement of its energy position with theoretical analysis of CTVE luminescence performed in the INDO calculations.[9]

C. Light absorption and second-harmonic generation

Let us discuss now the two experimental effects which could be interpreted as manifestations of the theoretically predicted CTVE phase. These are (i) dramatic shift with the temperature of the FLA edge in ferroelectric oxides, SBN and KTO, above room temperature (RT), and (ii) an appearance of a strong SHG signal in nominally pure incipient KTO and $SrTiO_3$ ferroelectrics at low temperatures, with a strong enhancement of this SHG signal in the external electric field.

(i) As was found,[19,38] the FLA edge above RT (Fig. 8) shifts in SBN by -1.3 meV/K (the largest magnitude found so far), revealed for the extraordinary light polarization. The value of the shift is -0.8 meV/K for KTO (both numbers are for an absorption value of 200 cm^{-1}). It should be noted that the FLA edge in both ferroelectric oxides obeys the usual Urbach law.

Such a strong FLA temperature shift could be explained as resulting from an additional in-gap band with a relatively small (0.1–0.2 eV) energy separation between the bottom of this new band and the top of the *standard* valence band of the perfect crystal. This additional band could be interpreted as the CTVE phase's valence band (Fig. 5). Its thermal population at $T > 300$ K with the following light-induced transitions to the CTVE-phase conduction band (which can overlap with the *normal* conduction band as discussed above)

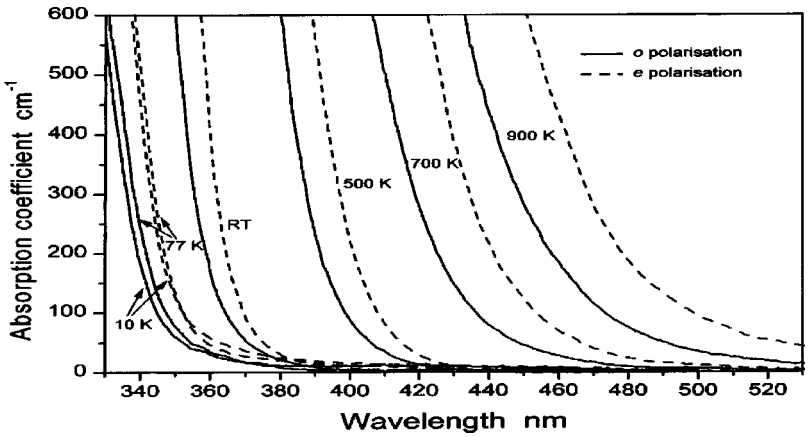

FIG. 8. Spectral and temperature dependence of the fundamental absorption coefficient for nominally pure SBN.

could lead to the observed strong red shift of the FLA edge. Moreover, this corresponds to the Urbach law which is observed experimentally.

(ii) It was found that the SHG signal in nominally pure KTO is unusually strong and increases unexpectedly sharply in an applied external electrical field. A strong thermal-treatment dependence of this signal is also very characteristic for this phenomenon. Namely, in nominally pure KTO and that doped with strong off-center Li^+ impurities, $K_{1-x}Li_xTaO_3$, the ratio $(\sqrt{n_{x=0.008}}\sqrt{\langle P\rangle^2_{x=0.008}})/(\sqrt{n_{x=0}}\sqrt{\langle P\rangle^2_{x=0}})$ is of the order of unity, in agreement with the SHG study.[39] Here $n_{x=0.008}$ and $\langle P^2\rangle_{x=0.008}$ are the concentration of Li^+ strong off-center impurity ions and the mean-square internal polarization induced by strong Li dipole impurities, respectively, both for $x=0.008$, whereas $n_{x=0}$, and $\langle P^2\rangle_{x=0}$ are the concentration of other-type dipoles (point dipoles or small polar clusters) in nominally pure KTO and mean-square internal polarization induced by them, respectively. This experimental result could be undestood if we assume that $n_{x=0}d_o^2 \approx n_{x=0.008}d_{Li}^2$ for a system of active dipole centers (or small polar clusters) with dipole moment d_o of the core of this defect in nominally pure KTO, on the one hand, and for a system of strong off-center Li^+ ions (with d_{Li} point dipole moment) in the $K_{0.992}Li_{0.008}TaO_3$. The latter means that nominally pure KTO contains active dipole centers (small polar clusters) which are as much effective in SHG creation as strong point dipole Li^+ centers, even for a non-negligible concentration of these impurity centers.

Moreover, the SHG electric field effect in nominally pure KTO is very strong,[40] probably due to the above-mentioned point dipoles or small polar clusters. For instance, the parameter $(\sqrt{\langle P^2\rangle_{x=0,E=160\ \mathrm{kV/m}}/\langle P^2\rangle_{x=0,E=0}}) \cong 17.3$, that is, much larger than unity. This means a huge polarizability of active dipole centers or small polar clusters.

Additionally, the reducing thermal treatment of samples leads to a strong increase of the SHG signal, while the oxidizing procedure leads to the opposite effect in nominally pure KTO. We can thus assume before microscopic model analysis that the number of active dipole centers (small polar clusters) in nominally pure KTO is increasing under reduction and is decreasing under its oxidation.

Last but not least, it should be stressed that the SHG temperature dependence for nominally pure incipient ferroelectric KTO (Ref. 40) can be fitted very well, assuming that an important role in SHG belongs to a soft polarization induced in the vicinity of point dipoles or of small clusters (with a radius less or the same order as the correlation radius of lattice polarization). Only for such *small* polar objects can we obtain a rather pronounced effect of a soft polarization region appearing in the surrounding of a dipole core and, as a result, the critical increase of induced polarization with the TO mode softening. This yields the SHG temperature dependence experimentally observed.[40]

All the above-considered experimental results could be explained in the framework of the model of small clusters of the CTVE phase. Indeed, a small and ferroelectrically ordered cluster of the CTVE phase (corresponding, for example, to a fragment of the CTVE phase in KTO (Fig. 4) with size less or the same order as the correlation radius of the lattice polarization) induces a strong polarization in its surroundings. This polarization critically increases nearby the soft mode condensation point, according to the Ornstein-Zernike law (similar to the semiphenomenological model[41]). This allows us to explain the observed SHG temperature dependence. Moreover, the polarization is rather high due to the contribution of the cluster core which contains ferroelectrically ordered CTVE's packed with a high density. In order to describe the SHG experimental results, the concentration of such small CTVE clusters should be $n_{x=0} \leqslant 10^{17}\ \mathrm{cm}^{-3}$.

In addition, the appearance of partly occupied $4d_{xy}$, $4d_{xz}$, and $4d_{yz}$ quasidegenerate atomic states of the electronic Nb polarons within the CTVE (with the energy splitting of the order of ~ 0.01 eV) induces a high polarizability of the CTVE in directions *perpendicular* to the CTVE main axis, due to the rotational degrees of freedom corresponding to the linear combinations of the wave functions of the two degenerated states, $(4d_{xz})+i(4d_{yz})$ and $(4d_{xz}-i(4d_{yz})$. This leads to the high polarizability of a whole ferroelectrically ordered cluster. This explains the unusually large effect of the applied electric field on the SHG efficiency.

Another important fact is related to the interfacial structure of the CTVE-phase cluster under consideration. Here a strong alignment of CTVE dipole moments induces inside a cluster a field compensation, which is due to appearance of

$(+2e)$-charged oxygen vacancies on the cluster interface towards which an internal cluster field is directed. As a result, the oxidation treatment decreases the number of CTVE-phase clusters but the reduction treatment leads to the opposite effect, which explains the experimentally observed SHG behavior.

VI. DISCUSSION AND SUMMARY

Two groups of results were presented in this study. First of all, we give theoretical computation evidence of the existence of CTVE and the CTVE phase in model perovskite-like crystals. Second, this is experimental evidence of the CTVE and CTVE-phase effects in the same type systems studied by optical methods. All these results prove the existence of CTVE's and the CTVE phase in partly covalent solids.

Note that CTVE states are not limited only to the cases which we considered here as examples. First of all, there exist CTVE clusters[3,42] trapped by charged impurities and by small polarons in SBN.[43] The CTVE cluster formation seems to be very important also from the point of view of their appearance in ferroelectric relaxors because the CTVE clusters can be polar and well reorienting. It is well known that reorienting polar clusters can control the phase transition phenomena in the relaxors. CTVE polar clusters in the relaxors can appear due to composition fluctuation effects. Namely, there are charge fluctuations in PMN-type relaxors and elastic field fluctuations in SBN-type relaxors. It should be underlined that recently the ferroelectric relaxor properties of SBN were indeed confirmed.[44] The CTVE-cluster role as polar-interacted clusters in PMN-type relaxors was already considered in Refs. 45 and 46.

Another aspect here is connected with the memory effect nature in real partly covalent solids with defects. Uncommon memory effects in α-quartz with Ge impurities under the conditions of x-ray-induced defects[47] and laser-induced site conversion with low-temperature memory in the BaFCl: Eu^{3+} crystals[48] were explained in the framework of the model of CTVE clusters induced by charged and elastic field defects.

Last but not least, the model of CTVE clusters induced by charged and elastic field defects had allowed us to propose a theory of multisite phenomenon formation[10] which was verified, for example, for the multisite structure induced by *large* and charged rare-earth impurities in lithium niobate crystal.[49]

We believe that the CTVE concept is effective for the understanding and description of many local and cooperative properties of real perovskites and ferroelectrics.

This study is supported in part by DFG, by DAAD, by NATO PST.CLG.977348, by NATO PST.CLG.977409, by NATO PST.CLG.977561, by Excellence Center for Advanced Materials Research and Technology (Latvia), by RFBR (01-02-17877, 00-02-16875), and by Russian Program on *Low dimension quantum structures*.

[1] V. M. Agranovich and A. A. Zakhidov, Chem. Phys. Lett. **50**, 278 (1977).
[2] P. Reineker and V. I. Yudson, Phys. Rev. B **63**, 233101 (2001).
[3] V. S. Vikhnin, Ferroelectrics **199**, 25 (1997); V. S. Vikhnin, Z. Phys. Chem. (Munich) **201**, 201 (1997).
[4] V. Vikhnin, Ferroelectr. Lett. Sect. **25**, 27 (1999).
[5] V. Vikhnin, H. Liu, and W. Jia, Phys. Lett. A **245**, 307 (1998).
[6] V. S. Vikhnin and S. Kapphan, Phys. Solid State **40**, 834 (1998).
[7] V. S. Vikhnin, H. Liu, W. Jia, and S. Kapphan, J. Lumin. **83-84**, 91 (1999).
[8] V. S. Vikhnin, H. Liu, W. Jia, S. Kapphan, R. I. Eglitis, and D. Usvyat, J. Lumin. **83-84**, 109 (1999).
[9] E. A. Kotomin, R. I. Eglitis, and G. Borstel, J. Phys.: Condens. Matter **12**, L557 (2000); R. I. Eglitis, E. A. Kotomin, and G. Borstel, Comput. Mater. Sci. **21**, 530 (2001).
[10] V. S. Vikhnin, A. A. Kaplyanskii, A. B. Kutsenko, G. Liu, J. Beitz, and S. E. Kapphan, J. Lumin. **94-95**, 775 (2001).
[11] R. I. Eglitis, N. E. Christensen, E. A. Kotomin, A. V. Postnikov, and G. Borstel, Phys. Rev. B **56**, 8599 (1997).
[12] R. I. Eglitis, A. V. Postnikov, and G. Borstel, Phys. Rev. B **54**, 2421 (1996).
[13] R. I. Eglitis, A. V. Postnikov, and G. Borstel, Phys. Rev. B **55**, 12 976 (1997).
[14] E. A. Kotomin, R. I. Eglitis, A. V. Postnikov G. Borstel, and N. E. Christensen, Phys. Rev. B **60**, 1 (1999).
[15] E. Stefanovich, E. Shidlovskaya, A. Shluger, and M. Zakharov, Phys. Status Solidi B **160**, 529 (1990).
[16] A. Shluger and E. Stefanovich, Phys. Rev. B **42**, 9664 (1990).
[17] A. Stashans and M. Kitamura, Solid State Commun. **99**, 583 (1996).
[18] V. S. Vikhnin, R. I. Eglitis, P. A. Markovin, and G. Borstel, Phys. Status Solidi B **212**, 53 (1999); R. I. Eglitis, E. A. Kotomin, and G. Borstel, J. Phys.: Condens. Matter **12**, L431 (2000).
[19] V. S. Vikhnin, S. Kapphan, and J. Seglins, Radiat. Eff. Defects Solids **150**, 109 (1999).
[20] K. M. Rabe and U. V. Waghmare, Phys. Rev. B **52**, 13 236 (1995).
[21] K. M. Rabe and U. V. Waghmare, J. Phys. Chem. Solids **57**, 1397 (1996).
[22] R. E. Cohen, Nature (London) **358**, 136 (1992).
[23] R. E. Cohen and H. Krakauer, Phys. Rev. B **42**, 6416 (1990).
[24] W. Zhong, D. Vanderbildt, and K. M. Rabe, Phys. Rev. Lett. **73**, 1861 (1994).
[25] R. Yu and H. Krakauer, Phys. Rev. Lett. **74**, 4067 (1995).
[26] W. Zhong, R. D. King-Smith, and D. Vanderbildt, Phys. Rev. Lett. **72**, 3618 (1994).
[27] P. Grenier, S. Jandl, M. Blouin, and L. A. Boatner, Ferroelectrics **137**, 105 (1992).
[28] W. Harrison, *Electronic Structure and Properties of Solids* (Freeman, San Francisco, 1980).
[29] S. A. Prosandeyev and A. I. Riabchinski, J. Phys.: Condens. Matter **8**, 505 (1996).
[30] P. Grenier, G. Bernier, S. Jandl, B. Salce, and L. A. Boatner, J. Phys.: Condens. Matter **1**, 2515 (1989).

[31] V. S. Vikhnin, S. Eden, M. Aulich, and S. Kapphan, Solid State Commun. **113**, 455 (2000).
[32] V. S. Vikhnin, S. E. Kapphan, and R. I. Eglitis, Ferroelectrics (to be published).
[33] E. Yamaichi, K. Watanabe, K. Imamiya, and K. Ohi, J. Phys. Soc. Jpn. **56**, 1890 (1987); E. Yamaichi, S. Ohno, and K. Ohi, Jpn. J. Appl. Phys., Part 1 **27**, 583 (1988).
[34] R. Leonelli and J. L. Brebner, Solid State Commun. **54**, 505 (1985).
[35] T. Hasegawa, M. Shirai, and K. Tanaka, J. Lumin. **87-89**, 1217 (2000); T. Hasegawa and K. Tanaka (unpublished).
[36] P. Camagni *et al.*, Radiat. Eff. Defects Solids **149**, 101 (1999).
[37] A. I. Popov and E. Balanzat, Nucl. Instrum. Methods Phys. Res. B **166-167**, 305 (2000).
[38] V. S. Vikhnin, S. Kapphan, and J. Seglins, J. Korean Phys. Soc. **32**, S621 (1998).
[39] auf der Horst Ch., J. Licher, S. Kapphan, V. Vikhnin, and S. Prosandeyev, Verhandl. DPG (VI) **35**, 413, DF 7.2 (2000); S. Eden, auf der Horst Ch., and S. Kapphan, J. Korean Phys. Soc. **32**, S411 (1998).
[40] P. Voigt and S. Kapphan, J. Phys. Chem. Solids **55**, 853 (1994).
[41] W. Prusset-Elffroth and F. Schwabl, Appl. Phys. A: Solids Surf. **51**, 361 (1990).
[42] V. S. Vikhnin and S. Kapphan, Ferroelectrics **233**, 77 (1999).
[43] V. S. Vikhnin, I. L. Kislova, A. B. Kutsenko, and S. E. Kapphan, Solid State Commun. **121**, 83 (2002).
[44] P. Lehnen, J. Dec, W. Kleeman, Th. Woike, and R. Pankrath, Ferroelectrics **240**, 281 (2000).
[45] V. S. Vikhnin, R. Blinc, and R. Pirc, Ferroelectrics **240**, 355 (2000).
[46] V. S. Vikhnin, R. Blinc, R. Pirc, and S. Kapphan, in *Fundamental Physics of Ferroelectrics*, edited by H. Krakauer, AIP Conf. Proc. No. 582 (AIP, Melville, NY, 2001), p. 144.
[47] V. S. Vikhnin and A. Leyderman, Ferroelectr. Lett. (to be published).
[48] V. S. Vikhnin, G. K. Liu, and J. V. Beitz, Phys. Lett. A **287**, 419 (2001).
[49] V. S. Vikhnin, A. A. Kaplyanskii, and A. B. Kutsenko, in Proceedings of the International Feofilov Symposium, Kazan, Russia, September, 2001 [Optics and Spectroscopy (to be published)].